

## Publication I

Leena Nurmi, Susanna Holappa, Hannu Mikkonen, and Jukka Seppälä. 2007. Controlled grafting of acetylated starch by atom transfer radical polymerization of MMA. *European Polymer Journal*, volume 43, number 4, pages 1372-1382.

© 2007 Elsevier Science

Reprinted with permission from Elsevier.

# Controlled grafting of acetylated starch by atom transfer radical polymerization of MMA

Leena Nurmi <sup>a</sup>, Susanna Holappa <sup>b</sup>, Hannu Mikkonen <sup>c</sup>, Jukka Seppälä <sup>a,\*</sup>

<sup>a</sup> *Laboratory of Polymer Technology, Department of Chemical Technology, Helsinki University of Technology, P.O. Box 6100, FIN-02015 HUT, Finland*

<sup>b</sup> *Laboratory of Forest Products Chemistry, Department of Forest Products Technology, Helsinki University of Technology, P.O. Box 6300, FIN-02015 HUT, Finland*

<sup>c</sup> *VTT Technical Research Center of Finland, P.O. Box 21, FIN-05201 Rajamäki, Finland*

Received 4 October 2006; received in revised form 15 January 2007; accepted 16 January 2007

Available online 31 January 2007

## Abstract

Graft copolymers of acetylated starch oligomer (AS) and poly(methyl methacrylate) (PMMA) were polymerized by atom transfer radical polymerization (ATRP). AS was converted to an ATRP macroinitiator by converting a part of the hydroxyl groups of AS to 2-bromoisobutyryl groups. Macroinitiators with varying degrees of substitution for the 2-bromoisobutyryl group were prepared. The polymerizations were conducted using CuBr/BiPy catalyst system, either in bulk or in 1:1 v/v THF solution. They proceeded with first-order kinetics and the molecular weights of the polymers increased linearly with conversion. Graft copolymers with different graft densities and graft lengths were prepared in a controlled manner. The hydrophobicity of these copolymers was studied by contact angle measurements.

© 2007 Elsevier Ltd. All rights reserved.

**Keywords:** Polysaccharide; Starch; Graft copolymer; ATRP

## 1. Introduction

Starch is one of the most abundant organic materials in nature. As a raw material it is renewable and economical. Starch and its derivatives have widespread industrial applications [1,2].

Starch consists of interconnected anhydroglucose units, each of which contains three hydroxyl groups. The properties of starch, such as its solubility in dif-

ferent solvents, can be routinely modified through converting the hydroxyl groups to other functionalities. Usually, this is done by either esterification or etherification reactions, but also grafting of starch with synthetic polymers by various methods has gained a lot of interest [1,3–6].

The most common way to synthesize starch based graft copolymers has been a radical polymerization with ‘grafting-from’ approach [3–6]. The initiating radicals have been formed on the starch chain either with chemical initiators or with irradiation. However, these methods suffer from low control of the graft density and length, and from the formation of unattached homopolymer.

\* Corresponding author. Tel.: +358 9 451 2614; fax: +358 9 451 2622.

E-mail address: [jukka.seppala@tkk.fi](mailto:jukka.seppala@tkk.fi) (J. Seppälä).

Recently, there has been a lot of research interest in a new field of controlled radical polymerization. At the moment several techniques enabling such polymerizations exist, of which ATRP (atom transfer radical polymerization) is one of the most commonly used [7]. The significant advantages of these polymerization techniques when applied in graft copolymerizations include the ability to polymerize grafts with controlled graft density and length, and narrow molecular weight distribution (MWD). In addition, homopolymer impurities are not formed in the polymerization [8].

Starch can be converted to an ATRP macroinitiator by converting part of the hydroxyl groups of starch to halide containing groups that are able to initiate the polymerization. There are several examples of polymerizations from saccharide-based initiators with ATRP technique. Several polymerizations have been conducted from low molecular weight mono- and disaccharides [9–11] and cyclodextrins [11–13]. Unmodified polysaccharides are often insoluble in most solvents, but there are reports of heterogeneous surface initiated ATRP conducted from cellulose and chitosan substrates [14–17] as well as from starch granules [18].

A few groups have grafted polysaccharides by homogeneous ATRP. Usually the polysaccharides have been modified by substitution in order to increase their solubility to typical ATRP solvents. Shen et al. polymerized methyl methacrylate onto cellulose diacetate [19] and methyl methacrylate and styrene onto ethyl cellulose [20]. Vlcek et al. [21] polymerized styrene, methyl methacrylate and butyl acrylate onto cellulose diacetate. They were also able to polymerize grafts with block structure. Recently, Bontempo et al. [22] were able to graft unmodified pullulan and dextran by ATRP using dimethylformamide/water mixtures as solvents. Their polymerization system was adjustable to many different monomers, and produced graft copolymers with good control.

However, to our knowledge, there are until now no reports of graft copolymerization by ATRP using dissolved, starch based materials as macroinitiators. In this study, we used ATRP to produce PMMA grafts onto acetylated starch oligomer in a controlled manner with varying graft densities and lengths. The graft copolymers were spin-coated onto silica surfaces from water dispersions as well as from THF solutions. The hydrophobicity of the produced graft copolymer surfaces was studied by contact angle measurements.

## 2. Experimental

### 2.1. Materials

Acetylated starch derivative (AS) with free hydroxyl groups, preferably at C-6 position of anhydroglucose unit, was prepared by using method described in the patent literature [23]. According to method native potato starch triacetate underwent acid catalyzed transglycosylation with ethylene glycol at 120–130 °C, which resulted in decrease in molecular weight and partial transesterification of C-6 acetyl with ethylene glycol. The degree of acetylation (number of acetyl groups per anhydroglucose unit) of the AS product was approximately 2.2.  $M_w$  of AS was ca. 50,000 g/mol and  $M_n$  4400 g/mol according to SEC measurement against PS standards. Before use the AS powder was dried under vacuum at 60 °C overnight.

Methyl methacrylate (MMA) (99% Aldrich) was dried with molecular sieves, passed through basic alumina to remove the inhibitor and stored under argon at –20 °C. CuBr (98% Aldrich) was stirred several times in glacial acetic acid, washed with ethanol and dried in vacuum. Tetrahydrofuran (THF) and pyridine were analytical reagent grades and dried with molecular sieves. 2-Bromo isobutyl bromide (BIB) (98% Aldrich), 2,2-bipyridine (BiPy) (99% Aldrich) and CuBr<sub>2</sub> (99% Aldrich) were used as received. Acetone, sulphuric acid, methanol and *n*-hexane were analytical grades and used as received.

### 2.2. Synthesis of the AS macroinitiator

AS was functionalized with different amounts of BIB. Typically, 5 g of AS (16 mmol of hydroxyl groups) was dissolved in 25 ml of THF. 9.9 ml of pyridine (122 mmol) was added. The solution was cooled to 0 °C, and subsequently 7.5 ml (61 mmol) of BIB was added dropwise. The reaction mixture was stirred for 1 h at 0 °C and then overnight at room temperature. The resulting salt was removed by centrifugation. The product was precipitated in hexane and purified by several repeated dissolutions in THF and precipitations in hexane. Finally, the product was dried in vacuum at 60 °C overnight. The degree of substitution was determined by <sup>13</sup>C NMR analysis.

### 2.3. Graft copolymerization

The polymerizations were conducted with a constant [MMA]/[Initiator group] ratio of 380:1. Since

a series of AS with different initiator group densities was used in polymerizations, the total amount of AS was varied in order to achieve this ratio.

For example, polymerization using AS functionalized with 0.09 initiator groups per anhydroglucose unit was conducted as follows: AS (530 mg, 0.19 mmol of initiator groups), CuBr (51 mg, 0.35 mmol) and BiPy (110 mg, 0.71 mmol) were placed in a dry Schlenk flask equipped with a magnetic stirring bar. The flask was evacuated and back-filled with argon three times. Degassed THF (7.6 ml) and degassed MMA (7.6 ml, 71 mmol) were added with gas-tight argon flushed syringes. The mixture was stirred until AS was dissolved. The flask was immersed in a pre-heated thermostated bath at 70 °C. A 0.2 bar argon overpressure was maintained within the flask throughout the polymerization. The polymerization was continued until the polymerization mixture became too viscous to be mixed.

During polymerization, samples were withdrawn at certain time intervals from the polymerization mixture using argon flushed syringes to follow the development of the molecular weight and monomer conversion. The molecular weight was determined by SEC and the monomer conversion was determined by  $^1\text{H}$  NMR, by comparing the relative ratios of MMA ( $=\text{CH}_2$ ) peaks (at 5.56 ppm and 6.10 ppm) and PMMA  $-\text{OCH}_3$  peak (at 3.60 ppm).

The polymers used in surface analysis were prepared otherwise as above, but they were quenched at certain time points, always before the viscosity of the mixture became high. In addition, after the polymerization they were diluted with THF and passed through basic alumina to remove the catalyst. The products were precipitated in hexane and purified by repeated dissolution in THF and precipitation in hexane.

#### 2.4. Hydrolysis of the AS backbone

The hydrolysis of the AS backbone was conducted according to method described by Shen et al. [19]. One gram of graft copolymer was dissolved in 30 ml THF and 20 ml acetone, then 4 ml of 70% sulphuric acid was added. The solution was refluxed at boiling point for 6 h. The residual polymer was precipitated in methanol.

#### 2.5. Graft copolymer characterization

Molecular weights and molecular weight distributions of the polymers were determined with res-

pect to polystyrene standards by size exclusion chromatography (SEC) at room temperature. The system was equipped with four Waters Styragel columns ( $10^2$ ,  $10^3$ ,  $10^4$  and  $10^5$  Å) and a Waters 410 differential refractometer. Chloroform was used as an eluent and was delivered at a flow rate of 1 ml/min.  $^1\text{H}$  NMR and  $^{13}\text{C}$  NMR spectra were recorded on a Varian Gemini 2000 300-MHz spectrometer in *d*-chloroform. Glass transition temperatures were measured with a Mettler Toledo DSC 821° differential scanning calorimeter.

#### 2.6. Graft copolymer surface preparation and characterization

The graft copolymer samples were applied onto hydrophilic silica surfaces either from 50 g/l THF solution or 50 g/l aqueous dispersion. The aqueous dispersions were prepared by a method described in the patent literature [24]. The method has been known to be suitable for most hydrophobic starches. The polymer particles <1000 nm in diameter were formed spontaneously when 2 g polymer samples dissolved in 100 ml of aqueous (20%) THF was rapidly diluted with 300 ml of water. THF solvent was evaporated by slight warming of dispersion at 40–60 °C. Solvent free polymer particle dispersion was concentrated through reversible flocculation by  $\text{Na}_2\text{SO}_4$ . The amount of salt used was 2% by weight of the water dispersion. After precipitation of particles the dispersion was further concentrated by centrifuge, diluted again to 250 ml volume with water and centrifuged 10 min 2000 rpm. The washing cycle by centrifuging was repeated twice to receive dispersion of purified micro-particles.

The hydrophilic silica was prepared from polished silicon wafers. The wafers were cut into slides and then cleaned (i) for 15 min in boiling mixtures of alkali and peroxide and (ii) for 15 min in boiling mixtures of acid and peroxide. The treatment induces the formation of hydroxyl groups on the silica surface. Spin coating was performed at spinning speed of 1500 rpm.

The effect of heating on surfaces spin-coated from aqueous dispersions was studied by heating the surfaces in an oven at 180 °C for either 5 min or 15 min. The silica slides were allowed to cool down at least for an hour before performing the contact angle measurements.

Dynamic contact angles on the graft copolymer layers were measured using a KSV CAM 200

computer-controlled video based instrument (KSV Instruments Ltd., Finland), which measures the development of the contact angle as a function of time. The measurements were made with MilliQ water. The measurements were repeated at least three times and the average value at time 10 s is reported.

The optical images were recorded with a digital camera combined to Leica MZ6 stereomicroscope.

### 3. Results and discussion

#### 3.1. Synthesis of the AS macroinitiators

A series of ATRP macroinitiators was produced by functionalization of AS. Part of the hydroxyl groups of AS were replaced with 2-bromo-isobutyryl groups, which are able to initiate polymerization by the ATRP mechanism. Three different macroinitiators (AS–BIB1, AS–BIB2, AS–BIB3) were prepared with different degrees of substitution for the initiator group. The degree of substitution (DS) is defined as the number of hydroxyl groups per anhydroglucose unit, which have been substituted by other groups. Since anhydroglucose units contain originally three hydroxyl groups, the maximum possible DS is three. However, since AS used in this study already contained acetyl groups with DS of 2.2, the maximum DS for the initiator groups (DS<sub>ini</sub>) was 0.8.

Macroinitiators were prepared by adding different amounts of BIB relative to the amount of hydroxyl groups of AS to the reaction. The macroinitiators are presented in Table 1. They enabled grafting with low (DS<sub>ini</sub> 0.02), intermediate (DS<sub>ini</sub> 0.09) and high (DS<sub>ini</sub> 0.76) grafting density. The achieved degrees of substitution correspond to 51.4, 10.5 and 1.3 anhydroglucose units per initiating site, respectively. One may notice that with AS–BIB3 approximately all remaining hydroxyl groups of AS have been converted to initiating sites.

DS<sub>ini</sub> was determined by <sup>13</sup>C NMR spectroscopy. The <sup>13</sup>C NMR spectrum of macroinitiator AS–BIB3 is presented in Fig. 1. The intensity of the acetyl group CH<sub>3</sub> carbon peak (9,10 in the figure) was compared with the intensity 2-bromo-isobutyryl group CH<sub>3</sub> carbon peak (12 in the figure). The DS<sub>ini</sub> and hence also the graft density in polymerization could easily be tuned by changing the ratio of BIB relative to OH groups in the reaction.

The  $M_n$  of the unreacted AS was approximately 4400 g/mol and  $M_w$  was approximately 50,000 g/mol according to SEC against PS standards. Due to the high polydispersity index (11.4), chain lengths of the macroinitiators varied from very short chains to very long ones. This means, that especially with AS–BIB1, where approximately only every 51st anhydroglucose unit was functionalized, it is apparent that part of the molecules at the low end of the molecular weight distribution remained unfunctionalized. On the other hand, at the high end of the molecular weight distribution all the macroinitiator chains were presumably functionalized many times, and the initiator density was the one described by DS<sub>ini</sub>.

#### 3.2. Graft copolymerization

A series of graft copolymers was polymerized using the three macroinitiators prepared. The polymerization series is presented in Table 2. The polymerizations were conducted with constant [MMA]/[CuBr]/[BiPy]/[Initiator] ratio of 380:1.9:3.8:1. In order to achieve this ratio, the total amount of AS added was varied since different macroinitiators contained initiator groups in different densities. All macroinitiators were grafted in bulk and in 1:1 v/v THF solution. The reason for the THF addition was to dilute the polymerization mixtures, some of which were already highly viscous in the beginning. THF has also been reported to increase MMA polymerization control with CuCl/

Table 1  
Macroinitiators

Macroinitiator	Mole ratio in reaction <sup>a</sup>	Degree of substitution <sup>b</sup> ( <sup>13</sup> C NMR)	Apparent $M_n$ <sup>c</sup> (SEC) g/mol
AS–BIB1	0.3	0.02	5900
AS–BIB2	1.0	0.09	7000
AS–BIB3	3.9	0.76	11,600

<sup>a</sup> Mole ratio of BIB/OH groups in reaction mixture.

<sup>b</sup> The amount of 2-bromo-isobutyryl groups/AS anhydroglucose unit.

<sup>c</sup> Determined with respect to linear polystyrene standards.

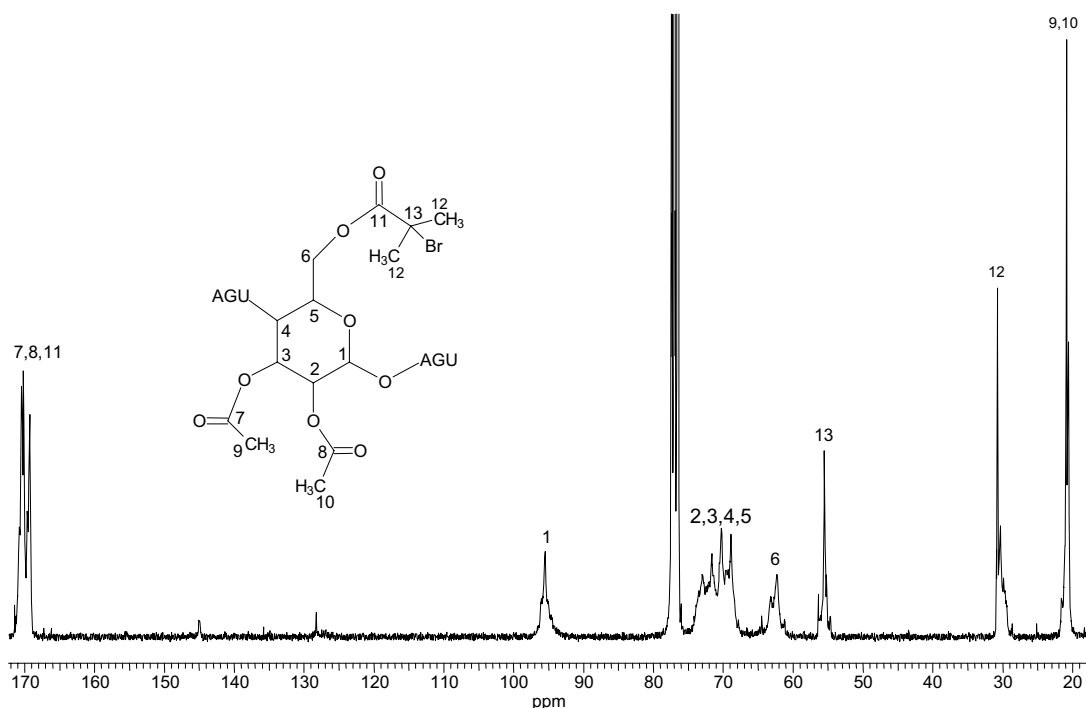


Fig. 1. 300 MHz <sup>13</sup>C NMR spectrum of AS macroinitiator (AS-BIB3) with assigned peaks.

Table 2  
Polymerization series

Polymerization	Solvent	DS <sub>ini</sub> of macroinitiator	<i>t</i> <sub>MP</sub> (min) <sup>a</sup>	Conversion at <i>t</i> <sub>MP</sub> (%)	<i>t</i> <sub>end</sub> <sup>b</sup>
AS-PMMA1	Bulk	0.02	5	8	10
AS-PMMA2	THF	0.02	70	35	120
AS-PMMA3	Bulk	0.09	20	18	30
AS-PMMA4	THF	0.09	33	30	40
AS-PMMA5	Bulk	0.76	15	12	17
AS-PMMA6	THF	0.76	21	13	26

<sup>a</sup> Time point, where the last conversion measurement was done.

<sup>b</sup> Time at the end of the polymerization. (Usually, the reaction mixture was so viscous that conversion measurement at this time point was unsuccessful.)

BiPy catalyst system due to the better solubility of the catalyst [25]. All the polymerization mixtures were partly heterogeneous with respect to the catalyst.

In most of the polymerizations the reaction mixtures were observed to form a highly viscous mass at relatively low conversions. The polymerizations were ended when the reaction mixture became too viscous to be mixed.

The reason for the observed viscosity behaviour is most probably the polyfunctionality of the growing graft copolymers. It makes them prone to intermolecular termination and therefore also to gelation [8,21,26–28]. The tendency for termination might

have been lower, if the [MMA]/[CuBr]/[BiPy]/[Initiator] ratio had been optimized. The used ratio (380:1.9:3.8:1) contained catalyst in an uncommonly high concentration with respect to initiator, even though it has been reported, that low catalyst concentration can suppress the termination reaction.

It has also been reported, that addition of CuBr<sub>2</sub> deactivator to the reaction can decrease the tendency for termination by decreasing the concentration of active radicals [26]. Therefore, we did an additional polymerization (AS-PMMA11) with one of the macroinitiators (AS-BIB2) to study this effect. The polymerization was conducted with [MMA]/[CuBr]/[CuBr<sub>2</sub>]/[BiPy]/[Initiator] ratio



Table 3  
Polymerization with added deactivator

Polymerization	Solvent	DS <sub>ini</sub> of macroinitiator	Conversion at $t_{\text{end}}^{\text{a}}$ (%)	$t_{\text{end}}$
AS-PMMA11	Bulk	0.09	31	33

<sup>a</sup> Time at the end of the polymerization.

of 380:1.3:0.6:3.8:1. The polymerization is presented in Table 3.

The kinetic curves of  $\ln([M]_0/[M])$  vs. time of all the polymerizations are presented in Fig. 2. It can be seen from the curves that the polymerization kinetics are first order when the conversion is low. The polymerization rates are similar in all the polymerizations. The polymerization AS-PMMA1 is not presented in Fig. 2, because the polymerization was fast and only one data point was measured (at 5 min the  $\ln([M]_0/[M])$  was 0.09). The rate was slightly lower in the polymerizations AS-PMMA5 and AS-PMMA6, which were done with the macroinitiator containing the highest initiator density. This could be due to their higher tendency to terminate by intramolecular radical coupling between neighbouring grafts [8].

The polymerization AS-PMMA11, which was done with lower initial CuBr amount and with added CuBr<sub>2</sub>, proceeded with approximately the same rate as the other polymerizations, possibly due to the low solubility of the deactivator [29].

The growths of the apparent molecular weights in polymerizations vs. conversion are presented in Fig. 3. The molecular weights seem to grow linearly with conversion, at least with the limited amount of data points available. However, also the intermolecular termination has an effect on the molecular weight of the samples, so no exact conclusions can be drawn from this dependency. The growth rate of  $M_n$  becomes higher with higher DS<sub>ini</sub> of the macroinitiator, as expected. The bulk and THF polymerizations from the same macroinitiator fit exactly to same lines when constant  $[MMA]/[CuBr]/[CuBr_2]/[BiPy]/[Initiator]$  ratio was used (polymerizations AS-PMMA2–AS-PMMA6), indicating equal initiator efficiency. Also AS-PMMA1 polymerization, which has not been presented in Fig. 3 since only one sample was measured, fits on the same line as AS-PMMA2 (at 8% conversion apparent  $M_n$  was 6700 g/mol). It is apparent, that polymerization control was similar in bulk and solution polymerizations, when constant polymerization conditions were applied. However, the AS-PMMA 11 polymerization, which was done with added

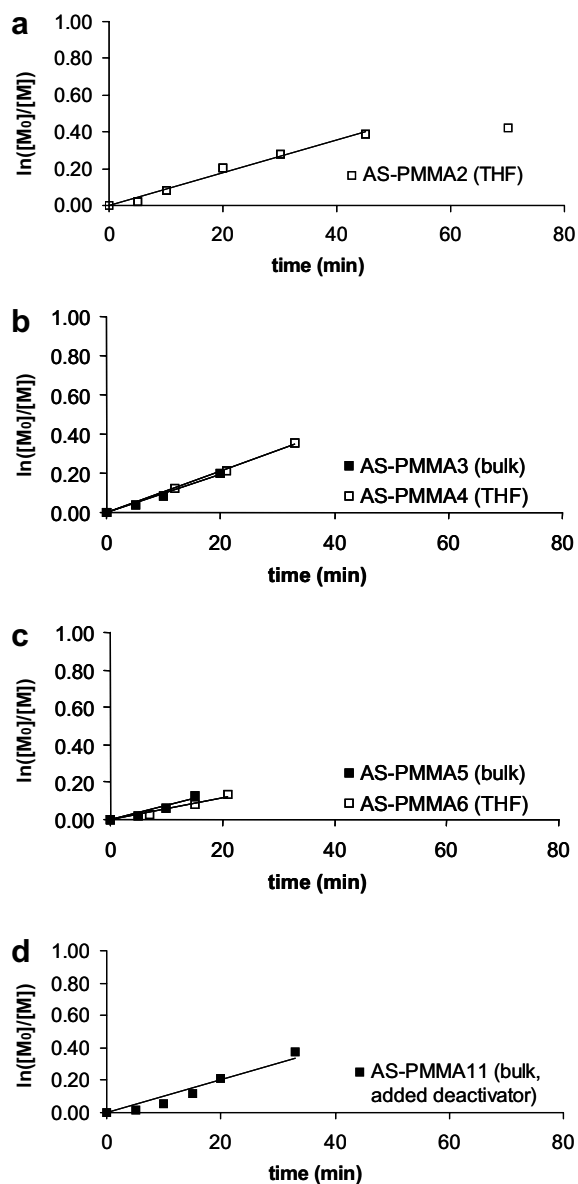


Fig. 2. Plots of  $\ln([M]_0/[M])$  vs. reaction times for all polymerizations: (a) solution polymerization with AS-BIB1 (DS<sub>ini</sub> = 0.02), (b) polymerizations with AS-BIB2 (DS<sub>ini</sub> = 0.09), (c) polymerizations with AS-BIB3 (DS<sub>ini</sub> = 0.76), (d) polymerization with AS-BIB2 (DS<sub>ini</sub> = 0.09) and added CuBr<sub>2</sub> deactivator.

deactivator, shows a slightly reduced  $M_n$  growth rate when compared to other polymerizations with

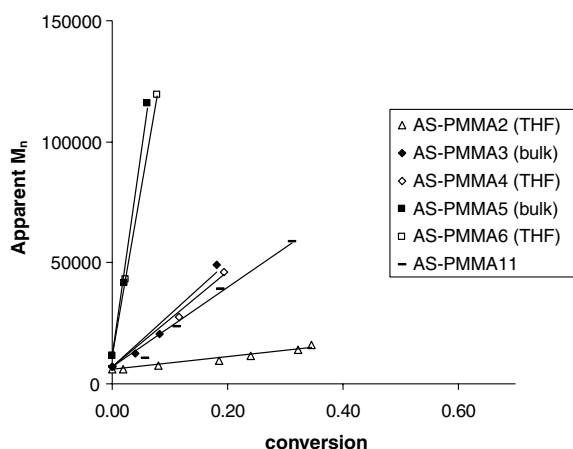


Fig. 3. Plots of apparent  $M_n$  (g/mol) vs. conversion in polymerizations. SEC measurement with linear PS calibration. AS-PMMA2: solution polymerization with AS-BIB1 macroinitiator ( $DS_{ini}$  0.02). AS-PMMA3 and AS-PMMA4: polymerizations with AS-BIB2 macroinitiator ( $DS_{ini}$  0.09). AS-PMMA5 and AS-PMMA6: polymerizations with AS-BIB3 macroinitiator ( $DS_{ini}$  0.79). AS-PMMA11: bulk polymerization with AS-BIB2 macroinitiator ( $DS_{ini}$  0.09) and added  $CuBr_2$  deactivator.

same  $DS_{ini}$  (AS-PMMA3 and AS-PMMA4). This might be due to decreased tendency for intermolecular termination, as discussed later.

The evolution of molecular weight distribution in AS-PMMA2, representing a polymerization with low graft density ( $DS_{ini}$  0.02), is presented in Fig. 4. At the low end of the MWD of the macroinitiator the probability of AS molecule being functionalized is low with this low  $DS_{ini}$ . Therefore part of the low molecular weight macroinitiator chains remain unreacted throughout the polymerization and can be seen as traces in the graft copolymer curve. The high molecular weight fraction of

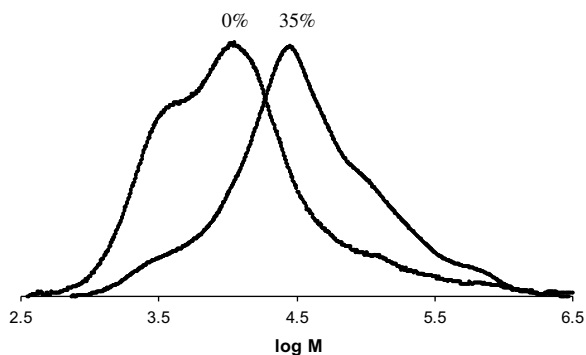


Fig. 4. Molecular weight distribution at different conversions in AS-PMMA2. ( $DS_{ini}$  was 0.02.)

the graft copolymer grows steadily in molecular weight and maintains the original MWD shape.

The evolution of the MWD of AS-PMMA4, representing a polymerization with intermediate graft density ( $DS_{ini}$  0.09), is shown in Fig. 5. Only slight traces of macroinitiator can be seen in the SEC curves. The graft copolymer curve follows roughly the shape of the macroinitiator at the low molecular weight end of the curve. However, at the high molecular weight end of AS-PMMA4 additional peaks seem to appear. The additional peaks are probably due to termination by intermolecular recombination.

The evolution of molecular weight distribution of the polymerization AS-PMMA6, representing a polymerization with high graft density ( $DS_{ini}$  0.76), is shown in Fig. 6. The curves move steadily towards higher molecular weight without any traces of macroinitiator. However, traces of intermolecular recombination can be seen also in this polymerization.

The evolution of molecular weight distribution of the polymerization AS-PMMA11 is shown in Fig. 7. When compared to polymerization AS-PMMA4 in Fig. 5, which was done with the same macroinitiator but without the deactivator addition, it can be seen, that the amount of intermolecular recombination at similar conversions has markedly decreased. Traces of intermolecular recombination are still clearly visible also in AS-PMMA11.

In order to study the actual grafts produced and get more information about the level of control in polymerization AS-PMMA11, the last sample of the polymerization was treated with 70% sulphuric acid to hydrolyze the AS backbone of the graft copolymer. The residual polymer was characterized with  $^1H$  NMR and SEC. The decrease in the intensities of AS backbone signals in the  $^1H$  NMR

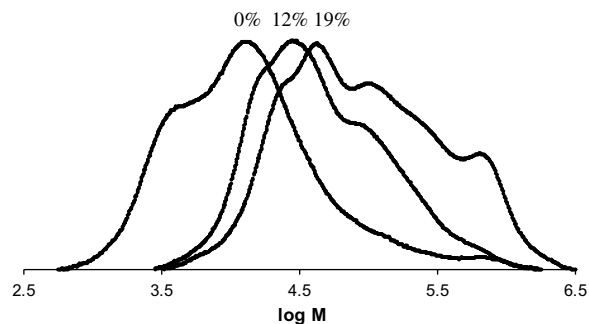


Fig. 5. Molecular weight distribution at different conversions in AS-PMMA4. ( $DS_{ini}$  was 0.09.)



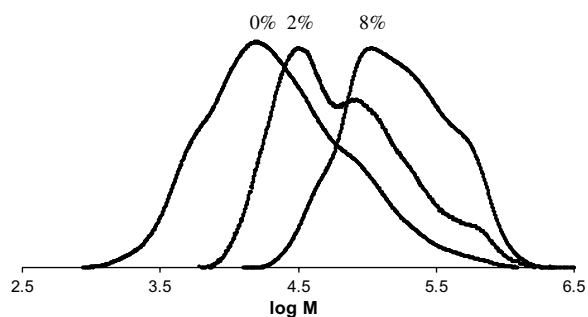


Fig. 6. Molecular weight distribution at different conversions in AS-PMMA6. ( $DS_{ini}$  was 0.76.)

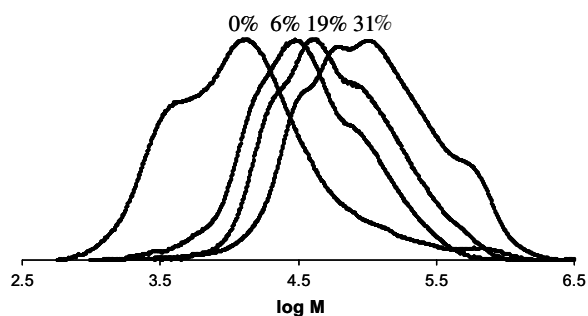


Fig. 7. Molecular weight distribution at different conversions in AS-PMMA11. ( $DS_{ini}$  was 0.09, deactivator had been added to polymerization).

analysis indicates fairly effective hydrolysis (Fig. 8). The SEC traces of the polymer before and after the hydrolysis are shown in Fig. 9. The polydispersity of the grafts was 1.33. The relatively low value confirms controlled polymerization.

### 3.3. Surface properties of the graft copolymers

Four graft copolymer samples (AS-PMMA7, AS-PMMA8, AS-PMMA9 and AS-PMMA10) were prepared for surface tests. The polymerizations were conducted with the original  $[MMA]/[CuBr]/[BiPy]/[Initiator]$  ratio without added deactivator (380:1.9:3.8:1). They were prepared by quenching the polymerization at different polymerization times corresponding to different PMMA/AS ratios in graft copolymers. The ratio between the PMMA and AS part in the graft copolymers was measured by  $^1H$  NMR spectroscopy by comparing the area of the peaks between 0.7 and 1.3 ppm ( $C-CH_3$  of PMMA) to the area of the peaks between 1.35 and 2.3 ppm ( $CH_3$  of AS and  $CH_2$  of PMMA). The samples are presented in Table 4.

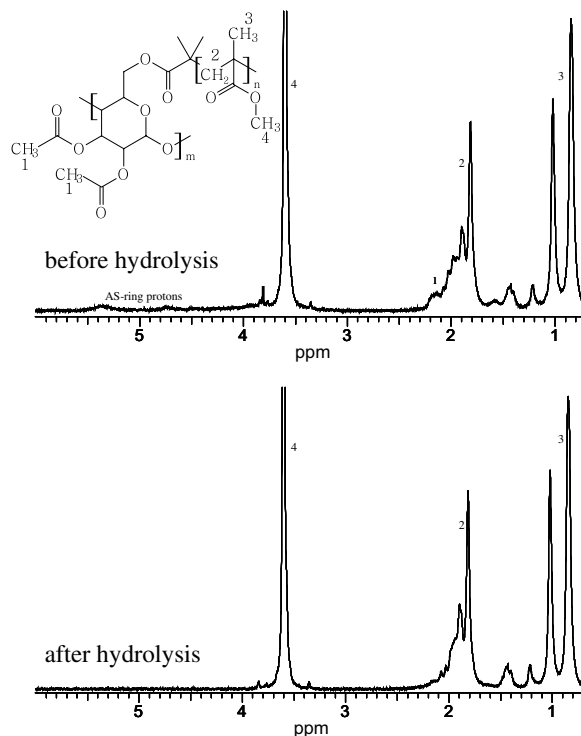


Fig. 8.  $^1H$  NMR spectra with assigned peaks from AS-PMMA11 graft copolymer and AS-PMMA11 residual polymer after the hydrolysis of AS chain.

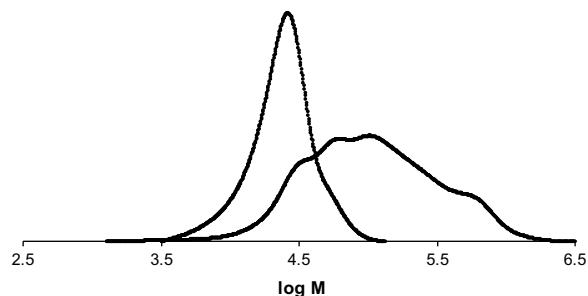


Fig. 9. SEC curves from AS-PMMA11 graft copolymer before and after the hydrolysis of AS chain.

The samples in Table 4 enable studying of the effect of graft density as well as PMMA/AS ratio on the surface properties. The samples AS-PMMA7 and AS-PMMA8 have the similar PMMA/AS ratios but different graft densities. The samples AS-PMMA8, AS-PMMA9, and AS-PMMA10 have the same graft density but they differ in PMMA/AS ratio.

The sample surfaces were prepared by spin-coating either from aqueous dispersions or THF

Table 4  
Copolymer samples in surface property tests

Sample	DS <sub>ini</sub> of the macroinitiator	Weight ratio PMMA/AS in copolymer	Theoretical graft length <sup>a</sup> (g/mol)
AS-PMMA7	0.09	0.7	1900
AS-PMMA8	0.02	0.6	6900
AS-PMMA9	0.02	1.4	16,600
AS-PMMA10	0.02	1.9	22,600

<sup>a</sup> The theoretical values have been calculated from the DS<sub>ini</sub> of the macroinitiator and the weight ratio of the components calculated from the <sup>1</sup>H NMR measurement.

solutions. The contact angles of water on the surfaces are presented in Fig. 10. They were compared to each other as well as to the contact angles on AS and PMMA homopolymers, which are 53° for AS (as measured from surface prepared by spin-coating from 50 g/l THF solution) and 69° for PMMA (as measured from surface prepared by spin-coating from 10 g/l toluene solution).

The surface set A in Fig. 10 is prepared from THF solutions of the sample polymers. The surface set B is prepared from their aqueous dispersions. The difference between these sets is clear. The contact angles on surface set A fit between the above mentioned contact angle values on homopolymers. The sample with the highest PMMA/AS ratio had

also the highest contact angle and the differences between samples were not large. On the other hand, the surface set B was hydrophilic with contact angles always below 35°.

Presumably the graft copolymers adopt in aqueous dispersion such a conformation, where the hydrophilic hydroxyl groups of AS are enriched on the particle surface and hydrophobic PMMA grafts remain hidden. This conformation is preserved during the spin-coating. The sample AS-PMMA7 had clearly the highest hydrophobicity of the set B. This can be due to the higher grafting density of the sample, which causes the hydroxyl groups of AS to be more hidden and PMMA grafts more exposed on the surface, respectively.

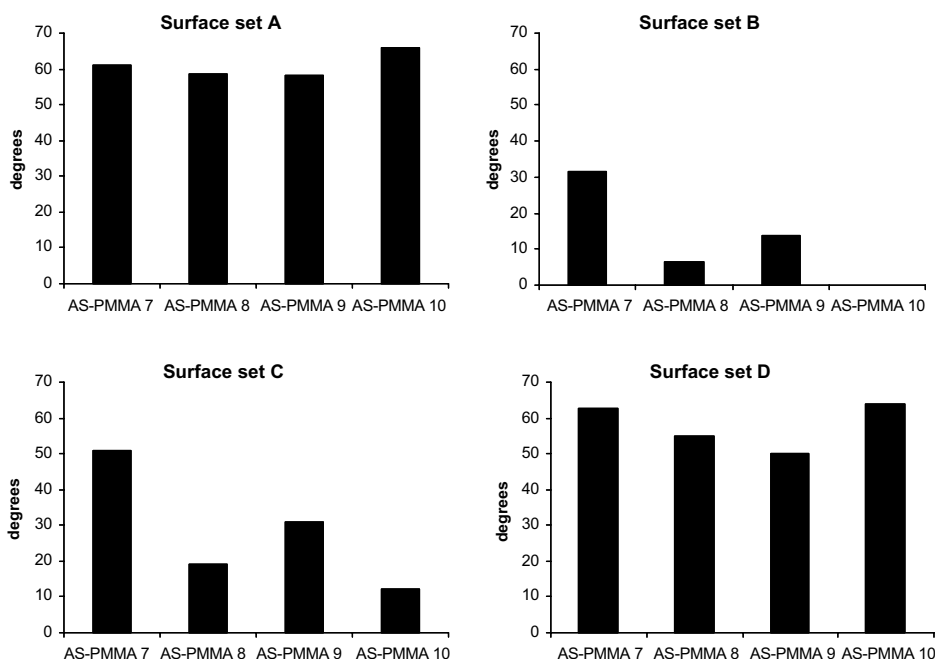


Fig. 10. Water contact angle values of spin-coated surfaces. Surface set A: prepared from THF solution, no heating. Surface set B: prepared from aqueous dispersion, no heating. The contact angle of sample AS-PMMA10 was too low to be measured. Surface set C: prepared from aqueous dispersion, 5 min heating in 180 °C after spin-coating. Surface set D: prepared from aqueous dispersion, 15 min heating in 180 °C after spin-coating.

However, it must also be noted, that the surfaces of surface set B appeared rather rough when studied with optical microscope. The roughness can also have an effect to the low contact angle values.

The surfaces prepared from aqueous dispersions were heated at 180 °C for varying time periods after the spin-coating (surface sets C and D) in order to study if that would change their conformation. The exposure to heating increased the contact angles of all surfaces clearly, even though the surfaces did not appear to be any less rough in the optical microscope. After 15 min of heating (surface set D) all surfaces had contact angles of at least 50°. The values are already near the contact angles of surfaces prepared from THF solutions (surface set A).

The glass transition temperatures ( $T_g$ ) of the homopolymer components of the graft copolymers were measured with DSC. The values were 120 °C for AS and 89 °C for PMMA. Therefore, even though  $T_g$  was not systematically measured for the graft copolymers, it is likely that the values are greatly under the 180 °C used in the heating. When the samples were heated above their  $T_g$ , they probably were able to rearrange in such a way, that the hydroxyl groups of AS were no longer enriched and PMMA grafts were no more hidden at the surface.

#### 4. Conclusions

The object of this work was to graft PMMA in a controlled manner onto acetylated starch by ATRP. AS macroinitiators with different degrees of substitution for the initiator groups (0.02–0.76) were prepared, resulting in tailored graft densities in graft copolymers. It was also possible to control the PMMA/AS ratio by quenching the polymerizations at determined polymerization times. The polymerizations showed living characteristics. Thus, the methods described allow the synthesis of AS-*g*-PMMA with tailored properties when conversion is kept low, even though the control of the polymerization was not perfect due to termination by recombination.

The synthesized graft copolymers were brought onto silica by spin-coating and the hydrophobicity of these surfaces was studied by contact angle measurements. The results indicate, that the composition and architecture of the copolymers (ratio of the components in graft copolymers and the graft density) as well as the way the surfaces are prepared (spin-coating from aqueous dispersion or THF solu-

tion) and treated (the exposure to heat treatment after the surface preparation) play a significant role in the hydrophobicity of the resulting graft copolymer surface.

In itself the possibility to prepare aqueous dispersions from these graft copolymers and the ability to use these dispersions to prepare surface coatings provides an easy and environmentally friendly method to be used in applications.

#### References

- [1] Daniel JR, Whistler RL. Starch. In: Ullmann's encyclopedia of industrial chemistry. Wiley-VCH Verlag GmbH & Co; 2002.
- [2] Maurer HW, Kearney RL. Opportunities and challenges for starch in the paper industry. *Starch/Stärke* 1998;50:396–402.
- [3] Fanta GF. Starch graft copolymers. In: Salamone JC, editor. *Polymeric materials encyclopedia*. Boca Raton; 1996. p. 7901–10.
- [4] Berlin AA, Kislenko VN. Kinetics and mechanism of radical graft polymerization of monomers onto polysaccharides. *Prog Polym Sci* 1992;17:765–825.
- [5] Jenkins DW, Hudson SM. Review of vinyl graft copolymerization featuring recent advances toward controlled radical-based reactions and illustrated with chitin/chitosan trunk polymers. *Chem Rev* 2001;101:3245–73.
- [6] Athawale VD, Rathi SC. Graft polymerizations: starch as a model substrate. *JMS – Rev Macromol Chem Phys* 1999; C39:445–80.
- [7] Matyjaszewski K, Xia J. Atom transfer radical polymerization. *Chem Rev* 2001;101:2921–90.
- [8] Pyun J, Kowalewski T, Matyjaszewski K. Synthesis of polymer brushes using atom transfer radical polymerization. *Macromol Rapid Commun* 2003;24:1043–59.
- [9] Haddleton DM, Edmonds R, Heming AM, Kelly EJ, Kukulj D. Atom transfer polymerisation with glucose and cholesterol derived initiators. *New J Chem* 1999;23: 477–9.
- [10] Bes L, Angot S, Limer A, Haddleton DM. Sugar-coated amphiphilic block copolymer micelles from living radical polymerization: recognition by immobilized lectins. *Macromolecules* 2003;36:2493–9.
- [11] Stenzel-Rosenbaum M, Davis TP, Fane AG, Chen V. Porous polymer films and honeycomb structures made by the self-organization of well-defined macromolecular structures created by living radical polymerization techniques. *Angew. Chem., Int. Ed.* 2001;40:3428–32.
- [12] Ohno K, Wong B, Haddleton DM. Synthesis of well-defined cyclodextrin-core star polymers. *J Polym Sci Part A: Polym Chem* 2001;2206–14.
- [13] Haddleton DM, Ohno K. Well-defined oligosaccharide-terminated polymers from living radical polymerization. *Biomacromolecules* 2000;1:152–6.
- [14] Carlmark A, Malmström E. Atom transfer radical polymerization from cellulose fibers at ambient temperature. *J Am Chem Soc* 2002;124:900–1.
- [15] Carlmark A, Malmström E. ATRP grafting from cellulose fibers to create block-copolymer grafts. *Biomacromolecules* 2003;4:1740–5.

- [16] Lindqvist J, Malmström E. Surface modification of natural substrates by atom transfer radical polymerization. *J Appl Polym Sci* 2006;100:4155–62.
- [17] ElTahlawy K, Hudson SM. Synthesis of a well-defined chitosan graft poly(methoxy polyethyleneglycol methacrylate) by atom transfer radical polymerization. *J Appl Polym Sci* 2002;89:901–12.
- [18] Liu P, Su Z. Surface-initiated atom transfer radical polymerization (SI-ATRP) of *n*-butyl acrylate from starch granules. *Carbohydrate Polym* 2005;62:159–63.
- [19] Shen D, Huang Y. The synthesis of CDA-*g*-PMMA copolymers through atom transfer radical polymerization. *Polymer* 2004;45:7091–7.
- [20] Shen D, Yu H, Huang Y. Densely grafting copolymers of ethyl cellulose through atom transfer radical polymerization. *J Polym Sci Part A: Polym Chem* 2005;43:4099–108.
- [21] Vlcek P, Janata M, Látalová P, Kríz J, Cadová E, et al. Controlled grafting of cellulose diacetate. *Polymer* 2006;47:2587–95.
- [22] Bontempo D, Masci G, De Leonardis P, Mannina L, Capitani D, Crescenzi V. Versatile grafting of polysaccharides in homogeneous mild conditions by using atom transfer radical polymerization. *Biomacromolecules* 2006;7:2154–61.
- [23] Mikkonen H, Peltonen S, Gädda T. Novel starch derivatives and a method for their preparation. WO03068823 2003.
- [24] Peltonen S, Mikkonen H, Qvintus-Leino P, Varjos P, Kataja K. Pigment and filler and a method of manufacturing it. EP1685185 2006.
- [25] Wang X, Luo N, Ying S. Controlled/living polymerization of MMA by heterogeneous initiation system (EPN-X-CuX-bpy). *J Polym Sci Part A: Polym Chem* 1998;37:1255–63.
- [26] Beers KL, Gaynor SG, Matyjaszewski K, Sheiko SS, Möller M. The synthesis of densely grafted copolymers by atom transfer radical polymerization. *Macromolecules* 1998;31:9413–5.
- [27] Masar B, Janata M, Látalová P, Netopilík M, Vlcek P, Toman L. Graft copolymers and high-molecular-weight star-like polymers by atom transfer radical polymerization. *J Appl Polym Sci* 2006;100:3662–72.
- [28] Maier S, Sunder A, Frey H, Mülhaupt R. Synthesis of poly(glycerol)-*block*-poly(methyl acrylate) multi-arm star polymers. *Macromol Rapid Commun* 2000;21:226–30.
- [29] Patten T, Matyjaszewski K. Atom transfer radical polymerization and the synthesis of polymeric materials. *Adv Mater* 1998;10:901–15.